ACS OMEGA

Open Access

http://pubs.acs.org/journal/acsodf

Article

Determination of the Lower Limit of Physical Properties of Tight Oil Reservoirs: A Case Study of the Lower Es_3 in the Jiangjiadian Area, Linnan Sag

Changcheng Han, Ming Qi,* Cunfei Ma,* Lanquan Zhao, Liqing Lei, Weiteng Kong, Zhipeng Li, Jian Li, Ning Lv, and Xi Cao

Cite This: *ACS Omega* 2023, 8, 35856−35865

Read Online

ACCESS | Metrics & More | Article Recommendations

ABSTRACT: The tight oil reservoir in Linnan Sag has great potential, a wide distribution range, and large total predicted resources. The rapid accumulation and burial of sediments in multiple source directions have resulted in the characteristics of low porosity and low permeability of the Lower Es_3 in the Jiangjiadian area, Linnan Sag. Based on conventional core analysis data, mercury injection data, and oil testing data, this paper comprehensively determines the lower limit of effective physical properties of reservoirs in the Jiangjiadian area of Linnan Sag and studies its main influencing factors. The results show that (1) the lower Es_3 reservoir in the Jiangjiadian area of Linnan Sag mainly develops feldspar sandstone and lithic feldspar sandstone. The porosity is mainly distributed at about 12%, and the permeability is mainly distributed at 0.3 mD; (2) based on the study of reservoir characteristics, the empirical statistical method based on core analysis data and the pore−permeability intersection method, the mercury injection parameter method based on test data, and the oil test verification method are used to comprehensively determine the lower limit of physical properties in the study area. The lower limit of porosity is 7.87%, and the lower limit of permeability is 0.16 mD; (3) sedimentation mainly affects the lower limit of physical properties by controlling reservoir lithology and pore structure. The existence of compaction and cementation in diagenesis will reduce the reservoir porosity and affect the lower limit of effective physical properties. The secondary dissolution pores formed by dissolution have a certain improvement effect on the effective physical properties of the reservoir.

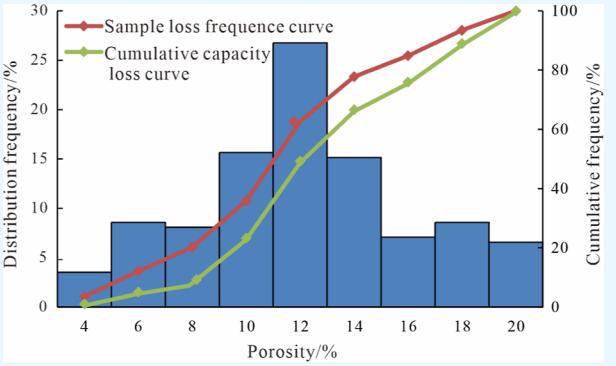

1. INTRODUCTION

Tight oil refers to oil stored in tight sandstone and carbonate reservoirs with permeability less than or equal to 0.1×10^{-3} μm^2.[1−3] Compared with conventional reservoirs, tight oil reservoirs have lower porosity and permeability. As one of the most important unconventional oil and gas resources in China's petroliferous basins, tight oil reservoirs have great potential for exploration and development.[4,5] Linnan Sag has the sedimentary characteristics of small area, multisource, near-source, and fast filling. The rapid accumulation of sediments in different directions and a series of diagenesis such as compaction, cementation, and dissolution after deep burial have resulted in the low porosity and low permeability of the Es_3 reservoir in Linnan Sag.[6,7] Tight oil in Linnan Sag has great development potential and wide distribution. The total predicted resources account for 87.6% of the total resources in Huimin Sag, but the actual proven reserves are only 0.2×10^8 t, which has great exploration and development prospects.

The lower limit of the effective physical property of a reservoir refers to the part of oil and gas accumulated in reservoir pores that can be mined out under the current industrial technology. Subject to the constraints of geological conditions and mining technology, the lower limit of the effective physical property of the reservoir is different in different regions.[8,9] The lower limit of physical properties is an important parameter for calculating the effective thickness and area of oil-bearing sand bodies, which is very important for the evaluation of reservoir quality and the calculation of reserves in tight oil, and it is also a key reference for the formulation of oil and gas field development plans.[10−12] At present, there is no fixed calculation method for determining the lower limit of the effective physical properties of reservoirs. Most of them are

Received: May 18, 2023
Accepted: September 6, 2023
Published: September 18, 2023

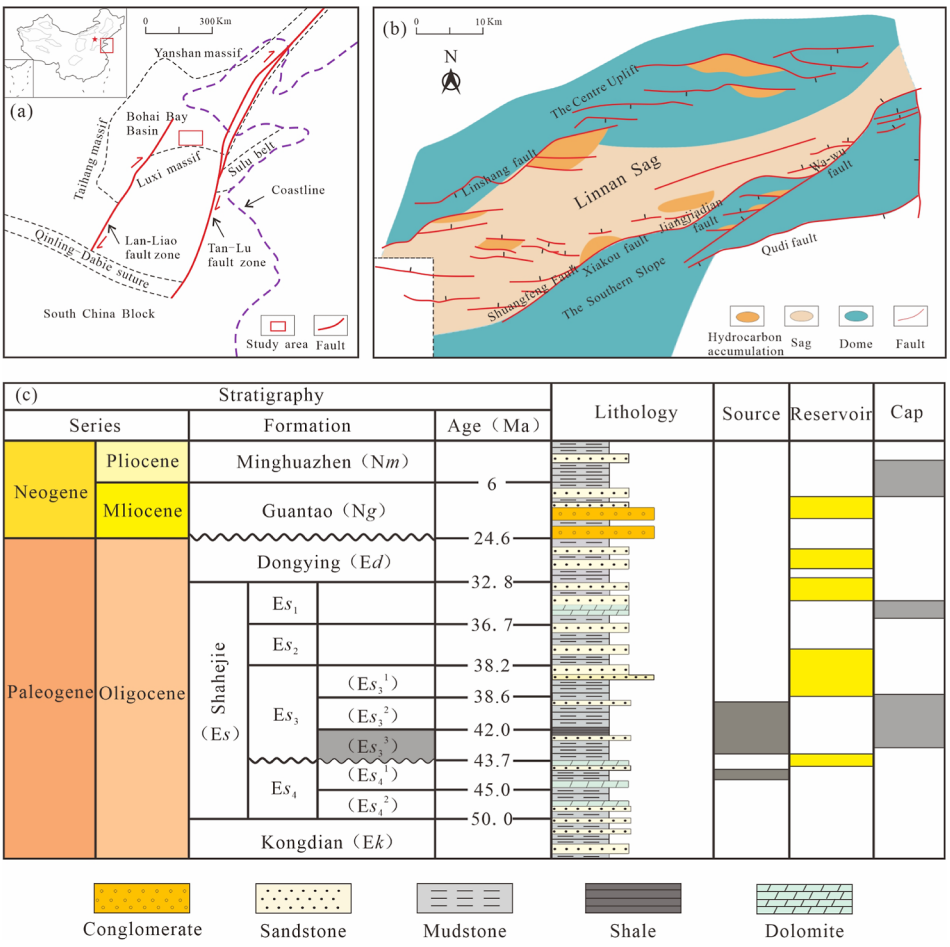

Figure 1. (a) Location map of Linnan Sag, (b) structural location of Linnan Sag, and (c) stratigraphic development map of Linnan Sag.

combined with the actual situation of the study area by using a combination of multiple methods.[8] The mainstream methods include static and dynamic types. Among them, the static method mainly includes empirical statistics, core oil occurrence analysis, porosity, and permeability intersection method, etc.[13,14] The dynamic method includes mercury injection parameter method, drilling fluid invasion calculation, etc.[15,16] Empirical statistics based on core test data are more suitable for a stable geological environment and a high-quality reservoir environment. The evaluation of the lower limit of effective physical properties of tight oil reservoirs has certain limitations due to the lack of verification of actual production data. These methods are mainly aimed at the same conventional reservoir to determine the unified lower limit of physical properties and are not fully applicable to tight oil reservoirs.[13,17] Therefore, it is urgent to combine various data to summarize the method for determining the lower limit of effective physical properties of tight oil reservoirs.

Tight oil reservoirs of lower Es_3 in the Jiangjiadian area of Linnan Sag have a large burial depth and low porosity and permeability. However, there is a lack of systematic research on the determination of the lower limit value of effective physical properties and their influencing factors. Based on the characteristics of tight oil reservoirs in the study area, this paper comprehensively uses the empirical statistical method based on core analysis and the porosity−permeability intersection method, the mercury injection parameter method based on test data, and the oil test method to calculate the lower limit of effective physical properties of reservoirs in the study area. Through the evaluation of the advantages and disadvantages of various calculation methods, the lower limit of effective physical properties of reservoirs in the study area is finally determined. Considering the influencing factors of the lower limit of effective physical properties of reservoirs in the study area from sedimentation and diagenesis. Finally, it provides a reliable basis for reservoir quality evaluation in the study area.

2. GEOLOGICAL SETTING

Linnan Sag is located in the southwest of Bohai Bay Basin, China, which belongs to the secondary tectonic unit in the middle of Huimin Sag (Figure 1a).[6] Linnan depression is connected to the Linyi fault in the north and the Xiakou fault in the south, forming a graben structure with an exploration area of about 1300 km^2 (Figure 1b).[18] Linnan Sag mainly experienced three tectonic development stages: the initial rift subsidence stage from the late Mesozoic to Eocene, the strong rift and subsidence stage from the late Eocene to Oligocene, and the post-rift subsidence from Miocene to the present.[18] The main development strata are the Paleogene Kongdian Formation, Shahejie Formation, and Dongying Formation; Guantao Formation and Minghuazhen Formation of Neogene. The Shahejie Formation is divided into Es_1, Es_2, Es_3, and Es_4 from top to bottom (Figure 1c). According to the difference in lithologic characteristics, the Es_3 is subdivided into upper, middle, and lower submembers. The lower Es_3 is the key oil-

https://doi.org/10.1021/acsomega.3c03379
ACS Omega 2023, 8, 35856−35865

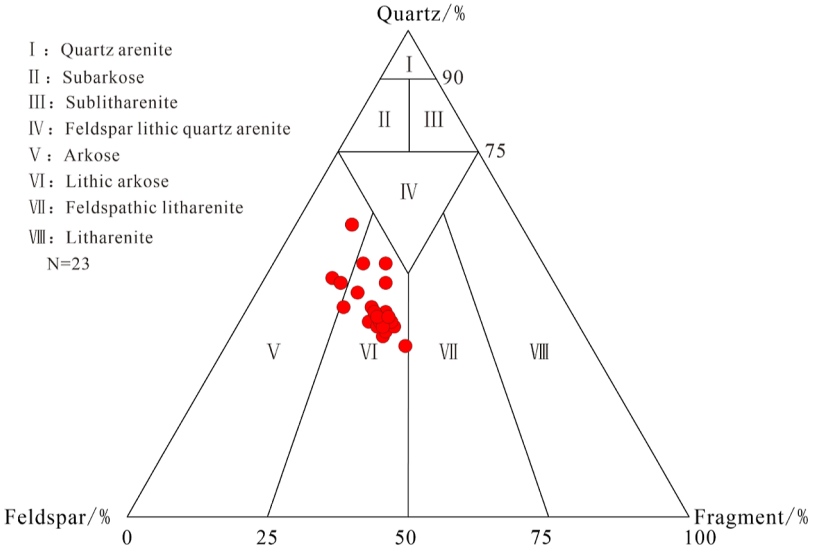

Figure 2. Triangle diagram of rock composition of the lower Es_3 in the work of Linnan Sag.

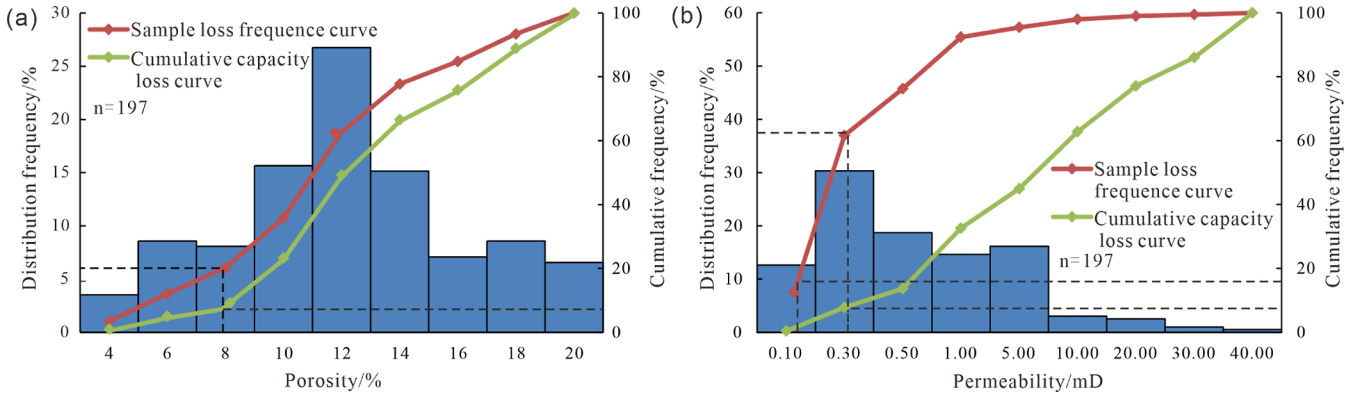

Figure 3. (a) Porosity distribution and cumulative productivity loss curve of the lower Es_3 in Linnan Sag; (b) permeability distribution and cumulative productivity loss curve of the lower Es_3 in Linnan Sag.

bearing section in this area, and the reservoir is buried deeply, with a maximum thickness of 500 m.[6,18] During the sedimentary period of the lower Es_3, the Jiangjiadian area mainly developed sedimentary microfacies such as delta front underwater distributary channel, estuary bar, and distal bar, and the lateral distribution of sand bodies was relatively stable.[19,20]

3. METHODOLOGY

In this paper, the core data of the coring wells in the Es_3 in the Jiangjiadian area of Linnan Sag are prepared and analyzed. The sample points cover the whole study area, mainly including the following contents:

(1) Bulk rock mineralogy: The bulk rock mineralogy test method can quantitatively determine the mineral content of the sample and the rock type of the study area. A total of 23 rock samples in the study area were selected, and the bulk rock mineralogy was performed using a RINT-TTR3 X-ray diffractometer. The scanning speed was 2°/min (2θ), and the scanning range was 5−45° (2θ). Before the analysis and testing, the rock samples need to be ground to 200 mesh. The mineral type and content are determined according to the strength of different mineral characteristic peaks, and finally, the mineral content of the rock should be determined. (2) Porosity and permeability measurement: 197 rock samples in the study area were selected for conventional physical parameter measurement. Rock samples were drilled along the horizontal direction of the core column, and then, the samples were ground into a small core cylinder with a diameter of 2.5 cm and a length of 5 cm. The porosity and permeability of the rock samples were measured using the CMS-300 type overburden pressure porosity and permeability meter. (3) Thin section preparation analysis: 30 rock samples in the study area were selected and ground into 0.03 mm thin sections. Before microscopic observation, blue epoxy resin was used to fill, and alizarin red and ferricyanide were used to stain, mainly highlighting the pore composition and carbonate cement type in the sample. A Carl Zeiss Axio Scope A1 optical microscope was used to observe the pore and mineral types in the sample. (4) SEM: scanning electron microscopy mainly observes the porosity and mineral content of rock samples at the micron−nanometer scale. Before observing under the microscope, it is necessary to pretreat the rock sample, cut it, and spray the Au element to improve its conductivity. A KYKY-2800 scanning electron microscope is used, with a resolution of 4.5 nm and a magnification of 15−250,000×. (5) High-pressure mercury intrusion test: 24 samples were tested by a YG-II high-pressure pore structure instrument. First, the rock sample needs to be dissected by an argon ion, then loaded into the core chamber, and sent to the vacuum pump for 1 h. Then, mercury should

https://doi.org/10.1021/acsomega.3c03379
ACS Omega 2023, 8, 35856−35865

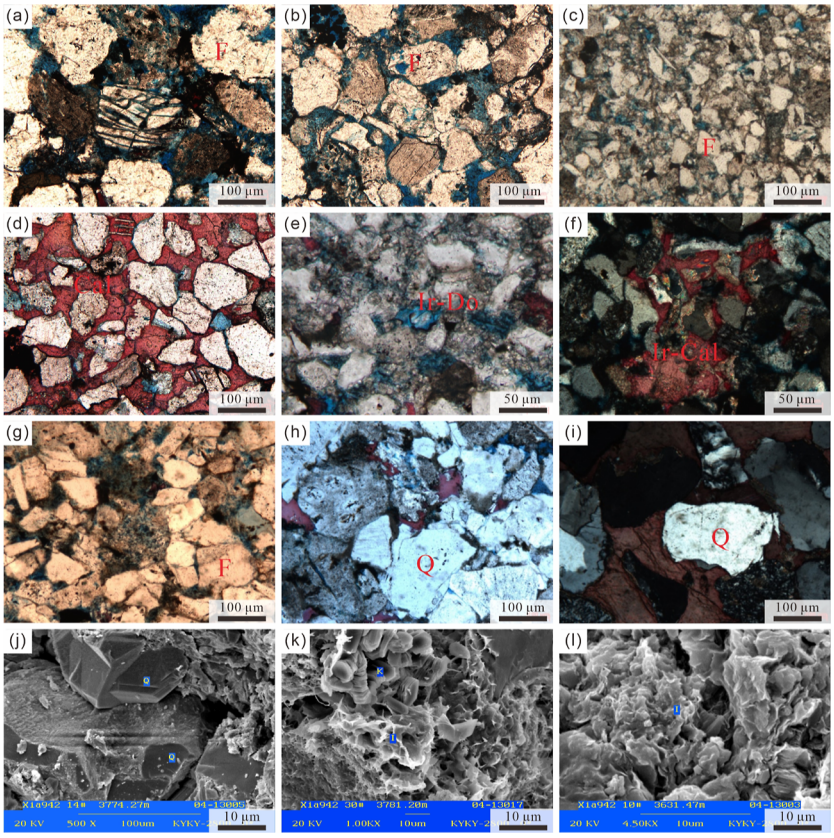

Figure 4. Microsedimentary characteristics of clastic rocks in the lower Es_3 in Linnan Sag: (a) compaction, brittle particles are fractured, X507, 3232.10 m, PPL; (b) compaction, debris particle line-convex contact, X507, 3232.10 m, PPL; (c) compaction, particle packing, X99, 4240.37 m, PPL; (d) calcite cementation replacement, X507, 3360.4 m, CPL; (e) iron dolomite cementation, X943, 3785.20 m, PPL; (f) iron-bearing calcite cementation, X507, 3360.4 m, CPL; (g) debris dissolution, X943, 3790.90 m, PPL; (h) quartz overgrowth edge dissolution, X943, 3791.60 m, CPL; (i) quartz cementation, quartz overgrowth edge, X943, 3791.50 m, CPL; (j) quartz cementation, quartz overgrowth, X942, oil-immersed siltstone, 3774.27 m, SEM; (k) clay mineral cementation, intergranular filling of kaolinite and illite, X942, oil spot siltstone, 3781.20 m, SEM; (l) clay mineral cementation, intergranular filling flake illite, X942, oil-immersed siltstone, 3631.47 m, SEM; F: feldspar; Q: quartz; Cal: calcite; Ir-Cal: iron calcite; K: potassium feldspar; I: illite; Ir-Do: ankerite; CPL: crossed-polarized light; PPL: plane-polarized light; SEM: scanning electron microscope.

be injected while the pressure is gradually increased, and the mercury pressure should be measured at 24 points to obtain the pressure parameters of each sampling point.

4. RESULTS

4.1. Basic Characteristics of the Reservoir. *4.1.1. Petrological Features.* The lithology types of tight oil reservoirs in the Es_3 of the Jiangjiadian area in Linnan Sag are complex and diverse. The whole rock mineral analysis results of 22 rock samples show that feldspar sandstone and lithic feldspar sandstone are mainly developed in the study area (Figure 2), and the compositional maturity of rocks is generally low. Quartz and feldspar content is higher, the average content can reach 45.50, 33.80%, and the composition of rock fragments is low, mainly metamorphic rock fragments, with an average content of only 2.70%.

4.1.2. Physical Characteristics. The physical properties of the reservoir directly determine the quality of the reservoir. The conventional physical property analysis results of 197 samples in the study area show that the maximum measured porosity of the core in the study area is 19.90%, the minimum value is 2.60%, and the average value is 11.28%. According to the porosity distribution histogram produced by the measured porosity of the core, the porosity is mainly distributed around 12% (Figure 3). The maximum measured permeability of the core is 26.778 mD, the minimum is 0.017 mD, and the average is 1.78 mD. According to the histogram of permeability distribution made by the measured permeability of the core, the permeability of the study area is mainly distributed around 0.300 mD (Figure 3), which belongs to the ultralow porosity, ultralow permeability−low porosity, and low permeability reservoirs.

4.1.3. Pore Structure. Both primary and secondary pores exist in the reservoir space of the study area (Figure 4a−l). Secondary pores mainly include secondary dissolution pores related to the dissolution of unstable components such as feldspar, quartz, and debris (Figure 4a,b). The secondary dissolution pores are mainly formed by the strong dissolution of the soluble components by the acidic fluid, which are the main migration channels of the fluid and belong to the main pore types in the study area. Intercrystalline pores (Figure 4b,c) developed between clay minerals, felsic minerals, calcite and dolomite minerals, and diagenetic microfractures filled with carbonate minerals. Primary pores mainly refer to the remaining intergranular pores after a series of diagenesis (compaction, cementation, and dissolution) experienced by the reservoir during formation (Figure 4c).

4.2. Determination of Lower Limit of Effective Physical Property of Reservoir. The lower limit of reservoir effective physical properties is not fixed; it will continue to

https://doi.org/10.1021/acsomega.3c03379
ACS Omega 2023, 8, 35856−35865

decrease with the improvement of reservoir evaluation methods or drilling and production processes.[21,22] At present, there is no fixed calculation method for determining the lower limit value of the effective physical properties of the reservoir. It is usually completed by combining various dynamic and static methods.[23] Based on the data of the study area, the empirical statistics method based on core analysis and the porosity and permeability intersection method, the mercury injection parameter method based on test data, and the oil test data are used to determine the lower limit of the effective physical properties of the reservoir in the Es_3 of Jiangjiadian area in Linnan Sag.

4.2.1. Empirical Statistical Method Based on Core Analysis. The empirical statistical method is based on the core test data. Through the measured porosity and permeability of the core, the lower limit of the effective physical property of the reservoir is determined according to the loss of the cumulative storage and permeability capacity of the low porosity and low permeability layers not exceeding 5% of the total cumulative amount. It has been widely used in the determination of the lower limit of the effective physical property of the reservoir.[24−26] The calculation formula is

$$Q_{\varphi_i} = \frac{\varphi_i H_i}{\sum_{i=1}^{n} \varphi_i H_i} \quad (1)$$

$$Q_{K_i} = \frac{K_i H_i}{\sum_{i=1}^{n} K_i H_i} \quad (2)$$

$$Q_{\varphi} = \sum_{i=1}^{n} Q_{\varphi_i} \quad (3)$$

$$Q_K = \sum_{i=1}^{n} Q_K \quad (4)$$

Q_{φ_i} is the oil storage capacity of the sample calculated according to the porosity value of the rock sample, %; Q_{K_i} is the oil storage capacity of the sample calculated according to the permeability value of the rock sample, %; H_i is the length of the sample, m; Q_{φ} is the cumulative oil production capacity of the sample calculated according to the porosity value of the rock sample, %; Q_K is the cumulative oil production capacity of the sample calculated according to the permeability value of the rock sample, %; n is the number of samples.

The effective porosity and permeability distribution histograms are made from the measured porosity and permeability data. The oil storage capacity and cumulative oil production capacity are calculated according to Formulas 1−4, and the cumulative frequency curve and cumulative productivity loss curve Q_{φ} and Q_K are plotted on the porosity and permeability distribution map (Figure 3).

According to the empirical statistical method, when the cumulative productivity loss frequency reaches 5.0%, the porosity is 7.8%, and the cumulative sample loss frequency is 6.2%, which is within the acceptable range. Therefore, 7.8% can be used as the lower limit of porosity calculated by the empirical statistical method in this area. Similarly, when the cumulative production loss frequency reaches 5%, the permeability value is 0.320 mD, and the cumulative loss frequency of the sample is 39.7%. Therefore, the cumulative loss of 15% of the permeability sample is selected as the limit, and the determined reservoir permeability is 0.140 mD.

4.2.2. Porosity−Permeability Intersection Method Based on Core Analysis. The porosity and permeability intersection method mainly determines the lower limit of the effective physical properties of the reservoir by making the intersection diagram of the measured porosity and permeability data of the core.[8] When the porosity data are small, the permeability increases slowly with the increase in porosity. When the porosity increases to a certain extent, the permeability increases exponentially with the increase in porosity. At this time, the porosity and permeability corresponding to the inflection point are the lower limit of the effective physical properties of the reservoir.[25] It can be seen from the cross-plot of porosity and permeability of the lower Es_3 in the Jiangjiadian area (Figure 5) that when the porosity value is less than 7.5%,

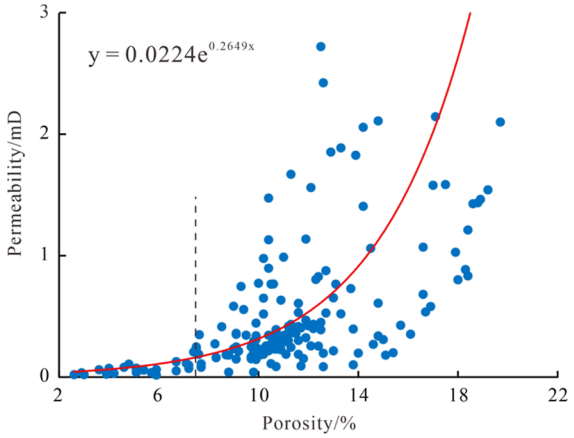

Figure 5. Cross-plot of the porosity and permeability of the lower Es_3 in Linnan Sag.

the permeability value increases slowly with the increase in porosity, but when the porosity value is greater than 7.5%, the permeability value gradually begins to increase sharply. The porosity at this time belongs to the effective porosity with a certain permeability.

Therefore, 7.5% can be used as the lower limit of porosity of effective reservoirs in the study area, and the lower limit of permeability of effective reservoirs is calculated to be 0.160 mD by Formula 5.

$$K = 0.0224\, e^{0.2649\varphi} \quad (5)$$

where K is permeability, mD; φ is porosity, %.

4.2.3. Mercury Injection Parameter Method Based on Test Data. The size of the pore throat usually controls the seepage capacity of reservoir fluid and directly affects the quality of the reservoir.[27] The displacement pressure obtained by mercury injection data mainly refers to the maximum pore throat pressure that needs to be overcome when the wetting fluid in the rock is replaced by the nonwetting fluid, that is, the minimum pressure when the water flooding fluid is used.[28] Therefore, the relationship between the displacement pressure and reservoir porosity determined by mercury injection data can be used to evaluate the effective physical properties of reservoirs.

According to the mercury injection data of 24 samples from 6 wells in the study area, the displacement pressure was calculated, and the relationship between the displacement pressure and porosity of the lower Es_3 reservoir in the Jiangjiadian area was obtained (Figure 6). When the porosity is

https://doi.org/10.1021/acsomega.3c03379
ACS Omega 2023, 8, 35856−35865

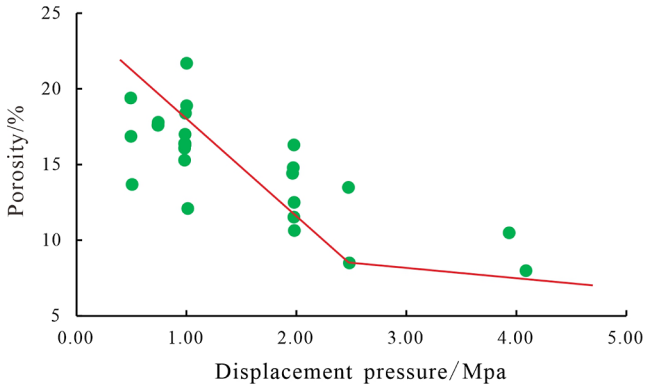

Figure 6. Relationship between displacement pressure and porosity of the lower Es_3 in Linnan Sag.

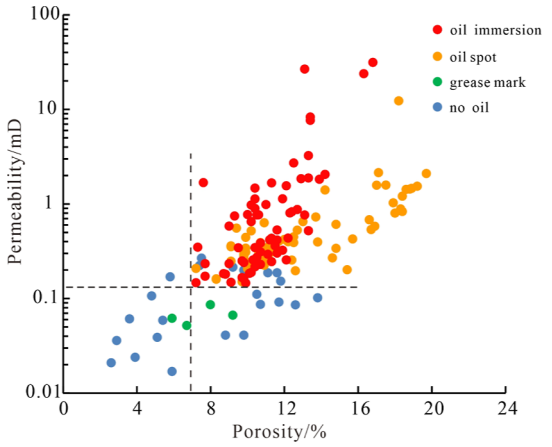

Figure 7. Relationship between oil-bearing property and core physical properties of the lower Es_3 in Linnan Sag.

less than 8.1%, the displacement pressure increases rapidly, indicating that it is difficult to become an effective reservoir when the reservoir porosity is less than 8.1%. Therefore, the lower limit of reservoir porosity in the lower Es_3 reservoir in Jiangjiadian is determined to be 8.1%. According to Formula 5, the lower limit of permeability is calculated to be 0.190 mD. The lower limit value of reservoir effective physical properties calculated by the mercury injection parameter method can make up for the lack of calculation results of actual geological conditions in the empirical formula method and the pore−permeability intersection method.

4.2.4. Oil Testing Data Method. The first-hand reservoir quality evaluation standard can be obtained through oil tests and production test data, which is very important for reservoir physical property evaluation.[29] Considering that the lower limit of effective physical properties calculated by the empirical statistical method based on core analysis and the mercury injection parameter method based on test data lacks the verification of field test data, the oil test data are introduced to obtain the lower limit of effective physical properties. Due to the limited oil test data in the study area, some core oil-bearing occurrence data are combined with the oil test data to make the pore−permeability cross-plot of the oil test section. The porosity and permeability values corresponding to the boundary position of the reservoir effectiveness are the lower limit values of the reservoir's effective physical properties. This method is more intuitive, simple, and convenient to operate. According to the porosity and permeability cross-plot of the test section (Figure 7), the lower limit of porosity can be determined to be 7.2%, and the lower limit of permeability is 0.160 mD.

5. DISCUSSION

5.1. Applicability of Lower Limit Determination Method of Effective Physical Properties. There are many methods for calculating the lower limit of effective physical properties of reservoirs, but each method has its applicable conditions and limitations.[30,31] Therefore, a complete discussion of the advantages and disadvantages of various methods will help us to determine the lower limit of effective physical properties of reservoirs in the study area more accurately.

The empirical statistical method and porosity−permeability intersection method based on core analysis are suitable for carrying out under the condition of having a large number of physical parameters. A large number of physical property analyses and test experiments are needed to obtain a large number of porosity and permeability data points. Among them, the empirical statistical method is not suitable for high permeability reservoirs because of the great influence of high permeability on the empirical statistical value and the human factors of the cumulative reservoir capacity limit that can be ignored when defining the lower limit of physical properties are large, which will cause large errors due to operators; the main limitation of the porosity and permeability intersection method is that there are great human factors in the definition of the production layer and the dry layer. The mercury injection parameter method based on test data mainly relies on the relationship between the displacement pressure and reservoir porosity determined by mercury injection data to evaluate the effective physical properties of reservoirs. The analysis of a large number of mercury injection data can objectively reflect the pore structure of the reservoir. Therefore, the combination of mercury injection data and physical property data can better determine the lower limit of physical properties of an effective reservoir. The oil test method and the oil-bearing occurrence method require that the test data include the reservoir section and the nonreservoir section, and need to meet the requirements of high accuracy of core and cutting oil-bearing description and oil test and production test, and the core porosity, permeability, mud logging description oil-bearing property must be consistent with the depth of the test section; otherwise, it is difficult to accurately determine the lower limit of the physical properties of the effective reservoir.

Through the analysis of the advantages and disadvantages of various methods for determining the lower limit of effective physical properties of reservoirs, it can be seen that in practical application, the actual geological conditions and analysis and test data of the study area must be fully considered and cannot be limited to one method of calculation. A variety of methods must be used to confirm each other to determine the lower limit of effective physical properties of reservoirs. Therefore, in this paper, through the empirical statistical method based on core analysis, the porosity−permeability intersection method, and the mercury injection parameter method based on test data and verified by the oil test method, based on the principle of statistics, the average value of the lower limit value of physical properties calculated by various methods is obtained. The lower limit value of effective porosity of the lower Es_3

https://doi.org/10.1021/acsomega.3c03379
ACS Omega 2023, 8, 35856−35865

reservoir of the Jiangjiadian area in Linnan Sag is 7.87%, and the lower limit value of permeability is 0.16 mD (Table 1).

Table 1. Lower Limits of Reservoir Properties Determined by Different Methods in the Lower Es_3 Reservoir of the Jiangjiadian Area in Linnan Sag

method	low limit of porosity/%	low limit of permeability/mD
empirical statistical	7.80	0.14
porosity−permeability intersection	7.50	0.16
mercury injection parameter	8.10	0.19
oil testing	7.20	0.16
Average	7.87	0.16

5.2. Influencing Factors of the Lower Limit of Reservoir Physical Properties. *5.2.1. Deposition.* As the main factor affecting the lower limit of effective physical properties of reservoirs, sedimentation is mainly affected by controlling reservoir lithology and pore structure.[32] The Es_3 in the Jiangjiadian area mainly develops delta front underwater distributary channels, mouth bars, and distal bar microfacies. The lateral distribution of sand bodies is relatively stable, and it is difficult to analyze the differences in the effective physical properties of reservoirs caused by different types of sedimentary microfacies. However, in different sedimentary microfacies, due to the difference in hydrodynamic force, the particle size and sorting of particles are different, which affects the lower limit of effective physical properties of reservoirs.[33,34] The rock particles of the lower Es_3 in the Jiangjiadian area of Linnan Sag are mainly fine sandstone and siltstone with fine grain size. According to the statistical results of the median particle size and sorting coefficient of the rock (Figure 8a,b), the porosity is positively correlated with the median particle size. The larger the particle size, the better the reservoir porosity; there is an exponential relationship between the reservoir porosity and the sorting coefficient. The better the sorting, the worse the porosity. The pore structure of the reservoir becomes better with the increase in particle size and poor sorting. The reservoir with a better pore structure has better physical properties and fluid seepage ability. Compared with the reservoir with a poor pore structure, the limit of the reservoir's physical properties is lower.

5.2.2. Diagenesis. In the process of reservoir formation, diagenesis affects reservoir quality by controlling pore structure,[35−37] which is the main controlling factor of the lower limit of effective physical properties of reservoirs. The present burial depth of the lower Es_3 in Linnan Sag is 1600−3500 m, which belongs to the stage of middle diagenetic evolution.[7] Compaction and cementation will have an impact on reservoir porosity, which is destructive diagenesis.[38] The dissolution is mainly caused by the dissolution of various soluble components such as feldspar and debris in the skeleton particles, which can increase the pore space of the reservoir and improve the quality of the reservoir.[38]

Compaction runs through the whole diagenesis process, resulting in the destruction of a large number of primary pores in the reservoir and the deterioration of the reservoir's physical properties. The microscopic sections of rock samples in the lower Es_3 in the Jiangjiadian area show that compaction is generally developed. The strong compaction leads to obvious plastic particles being fractured (Figure 4a), debris particle line-convex contact (Figure 4b), and a close accumulation of particles (Figure 4c). With the increase in the buried depth of the reservoir, the compaction effect is more obvious and the reservoir porosity is affected (Figure 9), thus affecting the lower limit of the effective physical properties of the reservoir.

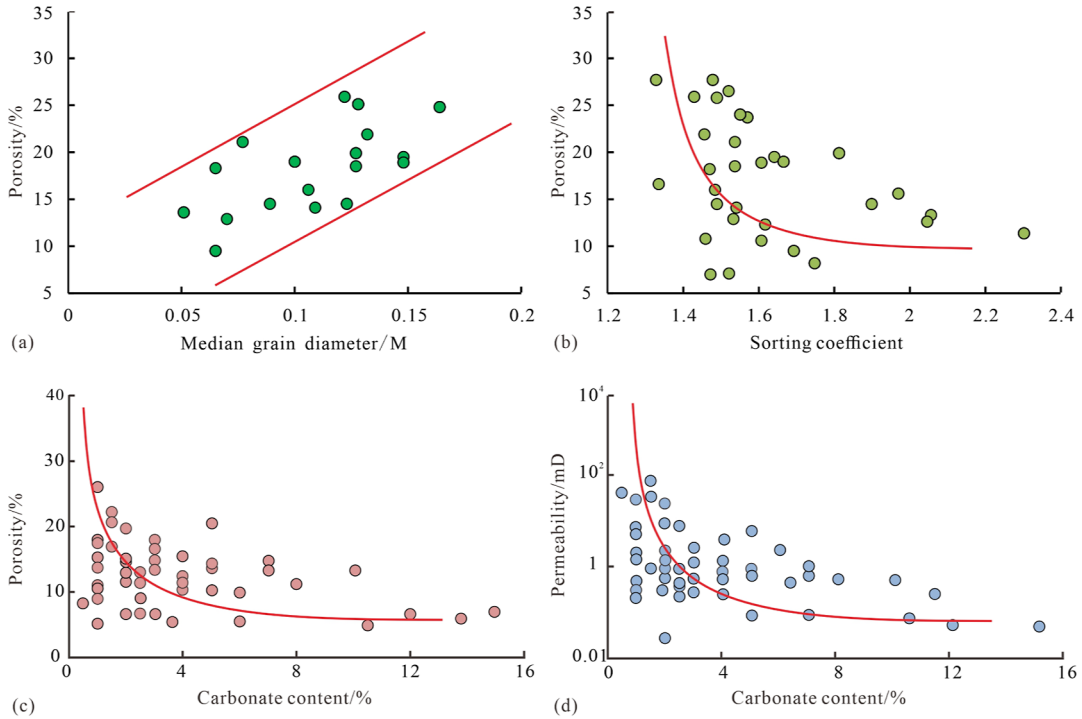

Figure 8. (a) Relationship between rock particle size median and porosity; (b) relationship between rock sorting coefficient and porosity; (c) relationship between carbonate content and porosity; (d) relationship between carbonate content and permeability.

https://doi.org/10.1021/acsomega.3c03379
ACS Omega 2023, 8, 35856−35865

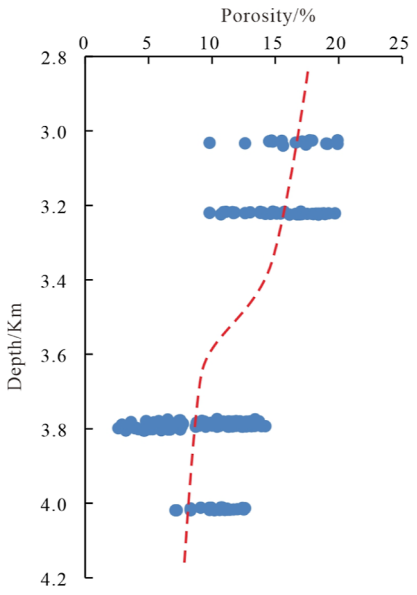

Figure 9. Variation curve of reservoir porosity with depth of the lower Es_3 in Linnan Sag.

The cementation in the study area is mainly carbonate cementation, followed by clay mineral cementation and quartz cementation. The carbonate cement such as calcite, ankerite, and ferrocalcite developed in the dissolution pores of the reservoirs in the Jiangjiadian area will seriously block the pore space (Figure 4d–f), thereby reducing the reservoir quality (Figure 8c,d). Intergranular filling kaolinite and flake illite will also fill pores to block the roar, resulting in a decrease in reservoir permeability. The phenomenon of quartz cementation is also common in the Jiangjiadian area (Figure 4j), but the integral number of quartz cementation objects is generally low, generally 0.5–3.0%, which has little effect on pores. The existence of cementation will reduce the porosity of the reservoir and affect the effective physical properties of the reservoir.

The existence of dissolution has a constructive effect on reservoir pores. The dissolution in the Jiangjiadian area is more common, mainly including the dissolution of easily soluble components such as feldspar, quartz, and cuttings (Figure 4g,h) and the dissolution of carbonate cement. The secondary dissolution pores formed by dissolution have a certain improvement effect on the effective physical properties of the reservoir.

6. CONCLUSIONS

(1) Based on core analysis data, the lithology of lower Es_3 in the Jiangjiadian area of Linnan Sag is mainly composed of feldspar sandstone and lithic feldspar sandstone. The porosity is mainly distributed in about 12%, and the permeability is mainly distributed in about 0.3 mD, which belongs to the ultralow porosity and ultralow permeability–low porosity and low permeability reservoir;

(2) Based on the study of reservoir characteristics, the empirical statistical method based on core analysis and porosity–permeability intersection method, the mercury injection parameter method based on test data, and the oil test verification method are used to determine the lower limit of effective physical properties of reservoirs in the study area. The lower limit of porosity is 7.87%, and the permeability is 0.16 mD;[21]

(3) Sedimentation and diagenesis are the main controlling factors affecting the lower limit of effective physical properties of reservoirs. The difference in sedimentation leads to a difference in rock particle size and sorting, which affects the porosity of the reservoir and the lower limit of effective physical properties of the reservoir. Compaction and cementation in diagenesis affect the effective physical properties of reservoirs as the main destructive diagenesis. The secondary dissolution pores formed by dissolution can improve the lower limit of reservoir physical properties.

AUTHOR INFORMATION

Corresponding Authors

Ming Qi – *College of Geology and Mining Engineering, Xinjiang University, Urumqi 830046, China; No. 6 Gas Production Plant, PetroChina Changqing Oilfield Company, Xi'an 710000 Shaanxi, China;* orcid.org/0009-0009-3610-3064; Email: 15029351462@163.com

Cunfei Ma – *School of Earth Science and Technology, China University of Petroleum (East China), Qingdao 266580 Shandong, China*; Email: mcf-625@163.com

Authors

Changcheng Han – *College of Geology and Mining Engineering, Xinjiang University, Urumqi 830046, China*

Lanquan Zhao – *Exploration and Development Research Institute of Shengli Oilfield, Sinopec, Dongying 257022 Shandong, China*

Liqing Lei – *Exploration and Development Research Institute of Shengli Oilfield, Sinopec, Dongying 257022 Shandong, China*

Weiteng Kong – *Shandong Energy Group South America Company Limited, Qingdao 257061 Shandong, China*

Zhipeng Li – *Exploration and Development Research Institute of Shengli Oilfield, Sinopec, Dongying 257022 Shandong, China*

Jian Li – *Exploration and Development Research Institute of Shengli Oilfield, Sinopec, Dongying 257022 Shandong, China*

Ning Lv – *National 305 Project Office, Urumqi 830000 Xinjiang, China*

Xi Cao – *Shandong Energy Group South America Company Limited, Qingdao 257061 Shandong, China*

Complete contact information is available at: https://pubs.acs.org/10.1021/acsomega.3c03379

Author Contributions

The authors contributed equally.

Notes

The authors declare no competing financial interest.

ACKNOWLEDGMENTS

The authors thank the National Natural Science Foundation of China (grant no. 42062010), construction project of teaching case base for professional degree graduate students (XJDX2023YALK17), and Xinjiang Uygur Autonomous Region Postgraduate Innovation Project (XJ2-23G112) and also thank anonymous reviewers for their constructive comments on this manuscript.

https://doi.org/10.1021/acsomega.3c03379
ACS Omega 2023, 8, 35856–35865

REFERENCES

(1) Wang, M.; Lu, S.; Huang, W.; Liu, W. Pore characteristics of lacustrine mudstones from the Cretaceous Qingshankou Formation, Songliao Basin. *Interpretation* **2017**, *5* (3), T373−T386.

(2) Suyun, H.; Zhu, R.; Wu, S.; Bai, B.; Yang, Z.; Cui, J. Profitable exploration and development of continental tight oil in China. *Pet. Explor. Dev.* **2018**, *45* (4), 737−748.

(3) Sun, L.; Zou, C.; Jia, A.; Wei, Y.; Zhu, R.; Wu, S.; Guo, Z. Development characteristics and orientation of tight oil and gas in China. *Pet. Explor. Dev.* **2019**, *46* (6), 1073−1087.

(4) Sun, L.; Tuo, J.; Zhang, M.; Wu, C.; Chai, S. Pore structures and fractal characteristics of nano-pores in shale of Lucaogou formation from Junggar Basin during water pressure-controlled artificial pyrolysis. *J. Anal. Appl. Pyrolysis* **2019**, *140* (JUN), 404−412.

(5) Zou, C.; Qiu, Z. Preface: New advances in unconventional petroleum sedimentology in China. *Acta Sedimentol. Sin.* **2021**, *39* (01), 1−9.

(6) Cao, Y.; Wang, X.; Wang, Y.; Yang, T.; Cheng, X.; Wang, S. Evolution of Diagenetic Fluids in Reservoirs of Esx3 in Jiangjiadian Area of Linnan Sag. *Xinjiang Pet. Geol.* **2017**, *38* (02), 127−132.

(7) Longwei, Q.; Zheng, S.; Fu, D.; Pan, Z.; Yang, S.; Qu, C. Controlling Factors Analysis and Quantitative Model of Shahejie 3rd Sandstone Porosity in Linnan Sag. *J. Jilin Univ., Earth Sci. Ed.* **2016**, *46* (5), 1321−1331.

(8) Liu, Z.; Shi, Y.; Zhou, J.; Wang, C.; Zhang, Y.; Zhang, P. Review and applicability analysis of determining methods for the lower limit of physical properties of effective reservoirs. *Prog. Geophys.* **2018**, *33* (03), 1102−1109.

(9) Wei, L.; Lingmei, N. Main controlling factors of formation and evolution of effective reservoir in tight sandstone: taking Bashijiqike Formation sandstone reservoir in Kuqa Depression as an example. *Fault-Block Oil Gas Field* **2020**, *27* (01), 7−12.

(10) Han, F.; Song, G.; Wu, Z.; Shen, X.; Han, F. Multi - attribute Fusion Prediction Technique for Tight Oil "Sweets. *Spec. Oil Gas Reservoirs* **2019**, *26* (01), 94−99.

(11) Lu, F.; Wang, J.; Zhang, J.; Luo, Z.; Shang, L.; Li, X.; Wu, K.; Su, H. Characteristics and lower limit of physical properties for reservoirs of 1st Member of Sangonghe Formation in Mosuowan area. *Fault-Block Oil Gas Field* **2021**, *3* (03), 300−304.

(12) Yongdong, Z.; Yongqiang, Z.; Hongqiang, M. Densification and diagenetic facies of Donghetang Formation sandstone reservoir in Bachu - Maigaiti area, Tarim Basin. *Pet. Geol. Exp.* **2019**, *41* (3), 363−371.

(13) Jing, F.; Luo, X.; Yang, Z.; Zhang, L.; Li, S.; Chen, Y.; Zeng, Y. Study on the porosity and permeability cutoffs of tight sandstones in shale stratum: Case study of Chang7Member of the Triassic Yanchang Formation, Ordos Basin. *Nat. Gas Geosci.* **2020**, *31* (6), 12−13.

(14) Shi, B.; Chang, X.; Yin, W.; Mao, L. Determination of Lower Limits of Critical Properties of Chang 8 Tight Sandstone Reservoirs, Zhenjing Block, Ordos Basin. *Acta Sedimentol. Sin.* **2020**, *38* (01), 231−243.

(15) Baoshou, Z.; Lu, X.; Sun, X.; Lu, H.; Lu, Y.; Tian, H. Study on the lower limit of physical properties of tight sandstone gas reservoirs in Dibei area, Tarim Basin. *Lithol. Reservoirs* **2015**, *27* (01), 81−88.

(16) Zhang, F.; Zhong, H.; Wei, D.; Zhang, F.; Liu, W.; Liu, W. Low limits of porosity and permeability for tight oil accumulations in the Chang 7 member, southeasterm Shaanbei Slope, Ordos Basin. *Nat. Gas Geosci.* **2017**, *28* (02), 232−240.

(17) Anda, Z.; Huifang, P. New methods to determine physical property lower limit of tight reservoir and their application. *Fault-Block Oil Gas Field* **2014**, *21* (5), 623−626.

(18) Yang, T.; Cao, Y.; Liu, K.; Tian, J.; Friis, H.; Zhou, L. Formation of zoned ankerite in gravity-flow sandstones in the Linnan Sag, Bohai Bay Basin, eastern China: Evidence of episodic fluid flow revealed from in-situ trace elemental analysis. *Mar. Pet. Geol.* **2020**, *113* (C), 104139.

(19) Du, S.; Qiu, L.; Nan, J.; Yang, Y. Reservoir features and controlling factors of the 3th members of Shahejie Formation in south slope of Linnan sag. *Sci. Tech. Eng.* **2018**, *18* (26), 68−76.

(20) Chai, J.; Wang, Y.; Wang, Z.; Wang, S.; Li, N.; Mi, L.; Zhou, L. Characteristics and Evolution of the Provenance Systems from the Paleogene Shahejie Formation in the Jiangjiadian Area, Huimin Sag. *Acta Sedimentol. Sin.*, 1−18.

(21) Yufeng, C.; Wang, G.; Sun, Y.; Wang, D.; Li, R. Methods of Cutoff Determination and Applicability Analysis in Low Porosity and Low Permeability Reservoir. *J. Southwest Pet. Univ.* **2016**, *38* (06), 35−48.

(22) Lu, Z.; Han, X.; Zhang, X.; Sun, T.; Wang, J.; Li, Y.; Zhao, H. Research status and outlook for methods of determining petrophysical property cutoffs. *J. China Univ. Pet.* **2016**, *40* (05), 32−42.

(23) Kang, T.; Wang, Y.; Shen, L.; Kang, H.; Zhu, L. Lower Property Limit and Controls on Clastic Reservoirs of First Member of Suhongtu Formation in Chagan Sag. *Unconv. Oil Gas* **2015**, *2* (05), 26−33.

(24) Hu, L.; Zhao, J. A discussion on the determination way to effective thickness of tight sandstone gas pools. *Nat. Gas Geosci.* **2013**, *24* (01), 69−77.

(25) Xueying, L.; Jiang, Y.; Liu, J.; Zahng, Y. Lower limits of porosity and permeability of tight sandstone gas reservoir in the middle-lower E_{S3} in Duzhai area, Dongpu Depression. *Geol. Sci. Technol. Inf.* **2017**, *36* (03), 182−188.

(26) Pengfei, Z.; Lu, S.; Li, W.; Hu, Y.; Xue, H.; Li, Q.; Zhang, H. Lower limits of porosity and permeability of shale oil reservoirs in the Xingouzui Formation, Jianghan Basin. *Oil Gas Geol.* **2016**, *37* (01), 93−100.

(27) Su, S.; Cheng, C.; Jiang, Z.; Shan, X.; Makeen, Y.; Gao, Z.; Zhu, R.; Lawal, M.; Ayinla, H. Microscopic pore structure and connectivity of lacustrine shale of the Shahejie Formation, Zhanhua Sag, Bohai Bay Basin. *Geoenergy Sci. Eng.* **2023**, *226* (226), 211800.

(28) Xiangzhen, M.; Liu, D.; Meng, W.; Leng, D.; Chen, L. Geological "Sweet - Spot" Evaluation of Chang - 7 Member Tight Oil in the Yanchang Formation of Southwestern Ordos Basin. *Spec. Oil Gas Reservoirs* **2018**, *25* (06), 90−95.

(29) Zhou, L.; Wang, Y.; Yu, W.; Lu, S. Classification assessment of tight sandstone reservoir based on calculation of lower and upper limits of physical properties—A case study of the tightsandstone reservoir in the 1st member of Funing Formation in Gaoyou Sag, North Jiangsu Basin. *Oil Gas Geol.* **2019**, *40* (06), 1308−1323.

(30) Yanquan, W.; Bian, W.; Liu, B.; Gu, G.; Sun, E.; Wang, P. Evaluation criterion and cut-off value of igneous rock reservoirs in Liaohe Basin. *J. China Univ. Pet.* **2016**, *40* (02), 13−22.

(31) Shiming, Z.; Wang, J.; Zhang, Y.; Zhang, X.; Zhang, T.; C, J. Determination of petrophysical property cutoffs of lacustrine dolomite intercrystalline pore reservoir in the Xiaganchaigou Formation, western Qaidam Basin. *Acta Pet. Sin.* **2021**, *42* (01), 45−55 + 118.

(32) Zeng, F.; Zhang, C.; Li, Z.; Zhang, G.; Zhang, C.; Wang, Y.; Sun, T.; Deng, Q. Controlling factors and distribution pattern of effective tight gas pools in blocky pyroclastic rocks in the Cretaceous Shahezi Formation in Wangfu gas field, southern Songliao Basin. *Oil Gas Geol.* **2021**, *42* (02), 481−493.

(33) He, J.; Fan, Z.; Song, H.; Li, K.; Kong, L.; Yao, J. Effective Reservoir Features and Distribution of the Badaowan Formation in the Baka Tight Sandstone Gas Field, Turpan-Hami Basin. *Sci. Tech. Eng.* **2015**, *15* (25), 108−114.

(34) Huang, Z.; Xu, Y.; Xue, G. Characteristics of retrogradational Fan Delta and Its Influencing Factors of Petrophysical Properties of the Zhuhai II Formation in Wenchang C Oilfield. *Sci. Tech. Eng.* **2017**, *17* (04), 182−188.

(35) Wang, Y.; Cheng, H.; Hu, Q.; Liu, L.; Hao, L. Diagenesis and pore evolution for various lithofacies of the Wufeng-Longmaxi shale, southern Sichuan Basin, China. *Mar. Pet. Geol.* **2021**, *133* (12), 105251.

(36) Baoquan, M.; Shumin, C.; Weilin, Y.; Chengyan, L.; Hong, Z.; Zhifeng, S.; Jiandong, Z.; Ya, W.; Shangxin, W.; Jingyan, W. Pore

https://doi.org/10.1021/acsomega.3c03379
ACS Omega 2023, 8, 35856−35865

structure evaluation of low permeability clastic reservoirs based on sedimentation diagenesis: A case study of the Chang 8 reservoirs in the Zhenbei region, Ordos Basin. *J. Pet. Sci. Eng.* **2021**, *196*, 107841.
(37) Si, S.; He, J.; Zhao, Y.; Er, C.; Bai, Y.; Wu, W. Diagenesis of tight sandstone and its influence on reservoir properties: A case study of Fuyu reservoirs in Songliao Basin. China. *Unconv. Resour.* **2023**, *3* (3), 84−92.
(38) Qi, M.; Han, C.; Ma, C.; Liu, G.; He, X.; Li, G.; Ya, Y.; Sun, R.; Cheng, X. Identification of Diagenetic Facies Logging of Tight Oil Reservoirs Based on Deep Learning—A Case Study in the Permian Lucaogou Formation of the Jimsar Sag, Junggar Basin. *Minerals* **2022**, *12*, 913.

https://doi.org/10.1021/acsomega.3c03379
ACS Omega 2023, 8, 35856−35865